

Effect of Climate Change on Design-Period Low Flows in the Mid-Atlantic US

Mary E. Schoen¹, Mitchell Small², Michael L. DeKay³, Elizabeth Casman⁴, Chuck Kroll⁵

¹PhD Candidate, Engineering and Public Policy, Carnegie Mellon Univ., 129 Baker Hall, Frew Street, Pittsburgh, Pa 15213. E-mail: mschoen@andrew.cmu.edu

²H. John Heinz III Professor of Environmental Engineering, Carnegie Mellon Univ., Civil & Environmental Engineering and Engineering & Public Policy, Porter Hall 119, Frew Street Pittsburgh, PA 15213. E-mail: ms35@andrew.cmu.edu

³Associate Professor, Engineering and Public Policy, Carnegie Mellon Univ., Hamburg Hall 2107B, Forbes Ave., Pittsburgh, Pa 15213. E-mail: deKay@andrew.cmu.edu

⁴Associate Research Professor, Engineering and Public Policy, Carnegie Mellon Univ., 129 Baker Hall, Frew Street, Pittsburgh, Pa 15213. E-mail: casman@andrew.cmu.edu

⁵Associate Professor, Environmental Resources and Forest Engineering, SUNY College of Environmental Science and Forestry, Syracuse, NY 13210. E-mail: cnkroll@esf.edu

Abstract

This study examines the relationship between changes in precipitation and temperature and the properties of low streamflow to estimate the potential impact of climate change on design-period low flows and associated Total Maximum Daily Loads (TMDLs) of primary pollutants. Stepwise linear regression is used for predicting the future low-flow statistic $Q_{7,10}$ using the physiographic and climatic characteristics of 160 watersheds in the Mid-Atlantic region of the United States. Based on four general circulation models' (GCMs') climate predictions of future increases in temperature and variable changes in precipitation, model results show a decrease in the $Q_{7,10}$ over the 21st century. Using Latin Hypercube sampling of parameter estimates, the fractional change in low flow and the resulting change in TMDL of a point-source primary pollutant are estimated for GCM climate predictions; for most predictions, a future reduction in contaminant load will be necessary to meet current water quality standards. Once GCM predictions improve, incorporating future climate scenarios in TMDL planning may preserve minimum water quality standards while avoiding a TMDL reallocation in the future.

Introduction

Future climate change has the potential to impact many aspects of water use and management. Five key water resource issues where impacts could occur include: ecosystem vulnerability; heavy precipitation and droughts; groundwater quality and quantity; competition for water supplies; and surface water quality (National Assessment Synthesis Team, 2001). These issues are interrelated, and while this study focuses on surface water quality, it also has implications for the other water resource issues.

Surface water quality is impacted by climate change through a combination of physical and biochemical processes involving changes in precipitation and air temperature. For example, increases in air temperature may induce a shift in aquatic biota by increasing surface water temperatures, resulting in decreased dissolved oxygen (DO) saturation concentrations and increased biochemical oxygen demand (BOD) (Morill, 2005; NAST, 2001). In a second example, increased winter temperature and precipitation may increase winter streamflow and reduce salinity levels in receiving estuaries (NAST, 2001). This study examines a separate potential impact of climate change on surface water quality: the impact of temperature and precipitation change on low streamflow (low flow) and the resulting change in the in-stream waste concentration of a pollutant.

The formulation of water quality management plans in the United States is driven by US EPA rules and guidance for the determination of Total Maximum Daily Loads (TMDLs) (National Research Council, 2001). As required by section 303(d) of the Clean Water Act (1987), each state must identify the waters which are not in attainment of water quality standards, not protecting a balanced wildlife population, or not supporting their designated use. For these impaired waters, each state must establish a TMDL which specifies the point and nonpoint source loadings which will bring the waterbody into compliance. For many primary pollutants, such as biochemical oxygen demand (BOD), dissolved solids, microbial pathogens, and acute toxics, critical loads are determined for a low-flow design period, during which the in-stream dilution provided by the waterway is minimum. The low-flow index most widely used for issuing of waste permit loads and considered in this study is the $Q_{7,10}$, or the 7-day annual minimum streamflow that is exceeded nine out of every ten years on average (Kroll *et al.*, 2004; Smakhtin, 2001; National Research Council, 2001). Any change in future climate that results in a significant reduction in low flows would invalidate assumptions made in TMDL calculations, with negative consequences for in-stream water quality.

Low flow is part of the natural, seasonal variation of a stream's flow when streamflow is supplied mostly by groundwater discharges during periods of little or no precipitation. Low flows are affected by changes in precipitation and temperature through ground water recharge, which is dependant on precipitation and evapotranspiration rates (Smahkin 2001). Climate observations over the past century and climate projections indicate possible significant shifts in temperature - and for some areas, precipitation - in this century (NAST, 2001), that may alter future low flows.

Over the 20th century, the average annual air temperature increased by 1° F in the United States and average national precipitation increased between 5 - 10%. Assuming that anthropogenic emissions of greenhouse gases such as CO₂ and methane are a discernable cause of the past century's climate change, and with continued gas emissions, climate change is likely to be larger in the future. The principal tools used to estimate possible future climate change, general circulation models (GCMs), generally agree that the climate in the next century will be warmer and experience more precipitation overall worldwide (NAST, 2001). However, there is disagreement regarding the specific location, timing and magnitude of possible future temperature increases. Furthermore, there is little agreement as to how precipitation will change on a regional level in the

future. Since both temperature and precipitation are key factors affecting groundwater recharge, it is uncertain how low flows might change in the future.

The next section of this paper describes the climate models used in this study, and how the model predictions might impact average streamflow and low flow. A low-flow model, previously fit by Kroll et al. (2004), is refit for 160 streamflow gauges in the Mid-Atlantic region, and the key climate inputs (temperature and precipitation) to the model are identified. The model is then applied using the predictions from four different GCMs as changes in model inputs. The implications for low-flow water quality and allowable primary pollutant TMDLs are subsequently derived.

Climate Models

The Mid-Atlantic region is expected to experience increases in both temperature and precipitation in the future, though the various GCMs differ in both the direction and magnitude of the predicted change for precipitation (IPCC, 2004). A further level of uncertainty is introduced as a result of differences in predicted greenhouse gas emissions for the next century. The Intergovernmental Panel on Climate Change, after grappling with this problem, produced a set of emission scenarios in the Special Report on Emission Scenarios (SRES) that the climate change community has reviewed. From that report, we chose emission Scenarios A2 and B2, which are derived from two separate storylines of the future. Scenario A2 has the underlying theme of strengthening regional cultural identities with high population growth and less concern for rapid economic development, and produces the highest emissions of CO_2 of all scenarios. An alternative Scenario B2 is based on a world where community initiative and social innovations find local solutions for economic, social and environmental sustainability (IPCC, 2000).

To find an approximate range of changes in air temperature and precipitation under these scenarios for the years 2010-2099, we used predictions from four coupled atmosphere-ocean GCMs: CSIRO from Australia's Commonwealth Scientific and Industrial Research Organization; HADCM3 from the Hadley Center for Climate Prediction and Research; CGCM2 from the Canadian Center for Climate Modeling and Analysis and; GFDL-R30 from the Geophysical Fluid Dynamics Laboratory. Together, the models give an idea of the range of changes in temperature and precipitation that could result from alternative future scenarios of economic activity and greenhouse gas emissions (IPCC, 2004).

The differences in climate predictions among models and scenarios are illustrated in Tables 1 and 2. These tables compare example seasonal precipitation and temperature change predictions for all four GCMs for both Scenarios A2 and B2 over the future time periods, 2010-2039, 2040-2069, and 2070-2099. The predictions include an absolute temperature change from baseline period 1961-1990 for average fall temperature; a percent change from baseline in spring precipitation; and a percent change from baseline in summer precipitation. In general, all models predict relatively large changes in climate in time period 2070-2099, and Scenario B2 predicts less severe change than Scenario A2.

Table.1. GCM Predictions for Future Seasonal Temperature and Precipitation Changes and Derived Predictions for Model Explanatory Variables Tmaxfal, Pavgapr, and Pminsum (Scenario A2)

	Sep-Nov Δ Temperature (K)	Mar-May Precipitation (% Change)	Jun-Aug Precipitation (% Change)
	Tmaxfal (K)	Pavgapr (% Change)	Pminsum (% Change)
Time Period: 2010-2039			
CSIRO	1.3	8.31	2.37
HADCM3	1.5	4.5	0.71
CGCM2	1.0	0.09	-0.66
GFDL-R30	1.8	3.6	-5.44
Time Period: 2040-2069			
CSIRO	2.7	9.24	3.74
HADCM3	3.0	4.41	4.5
CGCM2	2.4	1.41	-1.46
GFDL-R30	2.9	0.78	-6.43
Time Period: 2070-2099			
CSIRO	4.9	17.79	4.5
HADCM3	4.9	19.3	1.63
CGCM2	3.8	6.02	-5.08
GFDL-R30	4.4	11.62	-17.95

Table.2. GCM Predictions for Future Seasonal Temperature and Precipitation Changes and Derived Predictions for Model Explanatory Variables Tmaxfal, Pavgapr, and Pminsum (Scenario B2)

	Sep-Nov Δ Temperature (K)	Mar-May Precipitation (% Change)	Jun-Aug Precipitation (% Change)
	Tmaxfal (K)	Pavgapr (% Change)	Pminsum (% Change)
Time Period: 2010-2039			
CSIRO	1.8	5.16	5.31
HADCM3	1.5	2.21	4.21
CGCM2	1.3	-0.29	-1.5
GFDL-R30	1.2	5.55	-4.98
Time Period: 2040-2069			
CSIRO	2.8	6.59	7.54
HADCM3	2.2	8.07	3.56
CGCM2	1.7	2.84	-0.13
GFDL-R30	2.5	2.76	-9.87
Time Period: 2070-2099			
CSIRO	4.0	15.09	4.29
HADCM3	3.7	15.43	3.95
CGCM2	2.5	2.67	-0.41
GFDL-R30	3.4	2.68	-17.39

Hydrologic Models for Low Flow

Previous hydrologic case studies of basin response to climate change focus on estimating average streamflow response to changes in precipitation and temperature (Lettenmaier *et al.*, 1999; Nijssen *et al.*, 2001). These hydrologic case studies have similar conclusions. In general, future streamflows tend to be less sensitive to temperature than to precipitation, and changes in streamflow and runoff mostly follow changes in precipitation without moderation from evapotranspiration (Lettenmaier *et al.*, 1999). The largest anticipated changes in streamflows are those of snow-dominated basins where the temperature increases in winter months lead to higher winter streamflows and less spring runoff (Nijssen *et al.*, 2001).

Although there has been research on the effects of climate variability on runoff and mean flows, there has been little research on the impacts of climate change on other flow measures. Arnell (2003) addressed this research gap by investigating the impact of climate change on multiple flow indices using a dynamic flow model for six catchments in the United Kingdom. He concluded that climate change has a strong tendency to decrease low flow with apparent change predicted to occur by the 2020s. Eheart *et al.* (1999) also used climate scenarios to predict changes in low flow and found possible significant changes for the Midwest.

Numerous studies have focused on improving $Q_{7,10}$ regression models used at regional levels in the United States to estimate low flow from watershed and climatic characteristics (Dingman and Lawlor, 1995; Kroll *et al.*, 2004; Rifai *et al.*, 2000; Wiley and Curran, 2003; Zecharias and Brutsaert 1988). These studies focus on the selection of explanatory variables to maximize the predictive power of low-flow regression models for use on ungauged sites in a region (Smakhtin, 2001).

In our study, alternative models are fitted and compared for predicting the $Q_{7,10}$ for 160 gauged streams in the Mid-Atlantic US, and a model is selected for subsequent use in prediction. The model includes watershed physiographic features that are assumed to remain constant, and climate input variables that are assumed to change in the future. Although physiographic characteristics, such as landuse and landcover, are expected to change along with climate change, these characteristics are not included in the model due to the little land-use variation within the sample. The prediction thus uses differences in watershed features and climate inputs that occur *cross-sectionally* among the different streams in the region to predict changes expected to occur for each stream *longitudinally*, with modified future climate inputs. Particular care is made to identify the extent to which the predictions are interpolative, involving future climate conditions that are currently experienced by at least a subset of the current watersheds, verses extrapolative, projecting for conditions not currently experienced in the available dataset. Further insight into this issue is obtained by obtaining prediction intervals for the individual gauges' low-flow estimates that consider the additional error introduced when using values of predictor variables that are within, verses beyond, the range of the current data.

Streamflow Data and Watershed Characteristics

Streamflow Data

The $Q_{7,10}$ was calculated for each sample watershed by Kroll *et al.* (2004) using the United States Geological Survey's Hydro-Climatic Data Network (USGS HCDN) streamflow records. The USGS HCDN was created to investigate the response of surface-water to climatic variables; it contains streamflow records and physiographic characteristics spanning the years 1874 -1988 for over 1,500 streams across the United States. Streamflow records included in the HCDN database meet strict criteria, including a minimum of 20 water years of record with 95% of the daily mean discharge values assessed to be within 10% of the true value. In addition, HCDN stream gauges must have no flow restrictions, ground-water pumping, or significant land-use change during the period of record (Slack *et al.*, 1993).

Although the $Q_{7,10}$ is the most widely used low-flow index in the United States (Smakhtin, 2001), there is no consensus on the best estimation method (Kroll *et al.*, 2004). Kroll reported the $Q_{7,10}$ as the 10th percentile of the log-Pearson type III distribution of the 7-day annual minimum streamflows at each gauge.

Watershed Characteristics

The explanatory variables used in this study to predict the $Q_{7,10}$ include both watershed physiographic features and historic climatic variables estimated from weather gauges associated with or near the stream gauges. These characteristics are from a database created by Kroll *et al.* (2004) available at <http://www.esf.edu/erfeg/kroll/>. This database includes USGS HCDN characteristics as well as spatially processed digital information on the topography, meteorology, geology, and geomorphology of each HCDN watershed (Kroll *et al.*, 2004). In addition, the database includes numerous baseflow recession constants that are a function of the hydrogeologic characteristics of a catchment such as the porosity and hydraulic conductivity (Tallaksen, 1995).

The baseflow recession constant is an estimator of the daily percentage decline in streamflow during times of no surface runoff. Baseflow recession constants, which are dimensionless, have a range of 0 - 1 with 1 indicating the slowest decline. The recession constant used in this study was calculated using Method 5 outlined in Vogel and Kroll (1996). This method uses streamflow records as input to a least-squares estimator derived from the continuity equation when outflow from a watershed is linearly related to basin groundwater storage (Kroll *et al.*, 2004).

To create the spatially processed characteristics, Kroll (2004) used a 1 km digital elevation model to delineate watershed boundaries for each HCDN watershed. The watershed characteristics were based on summary statistics of digital grids within the delineated boundaries. Those grids include the United States Geological Survey 30 arc sec (~ 1 km) Hydro 1 K digital elevation model (DEM); the 1 km U.S. Department of Agriculture (USDA) State Soil Geographic grids (STATSGO); a 40-year monthly time series of the Spatial Climate Analysis Service (PRISM) 0.5° (~49km) orthographically

weighted precipitation and maximum and minimum temperature; and PRISM 2.5 arc min (~4km) average monthly and annual precipitation grids (Kroll *et al.*, 2004).

A total of 34 candidate variables were evaluated for inclusion in the model, including the baseflow recession constant, nine watershed physiographic variables, and 24 meteorological variables involving monthly or seasonal temperature and precipitation. Table 3 lists the 8 variables that were eventually included in the alternative models (the $Q_{7,10}$ for each gauge and seven explanatory variables) using the stepwise regression methods described in the following section. The explanatory variables include four watershed physiographic features, the baseflow recession constant (Kb2); the drainage area (DA); the mean basin elevation (Elev1); and the soil organic matter content (OMH), and three climatic variables: the 10th percentile of summer monthly precipitation (Pminsum), the average April precipitation (Pavgapr), and the 90th percentile of fall monthly temperature (Tmaxfal). Table 3 also shows the range and mean value of each of these variables for the 160 stream watersheds included in this study.

Table.3. Model Variables and Sample Characteristics (n=160)

Variable	Description	Units	Minimum	Mean	Maximum
$Q_{7,10}$	10th percentile of the distribution of 7-day annual minimum streamflows	m ³ /s	0.00	0.93	42.9
Kb2	Baseflow recession constant		0.903	0.947	0.976
DA	Drainage area	km ²	6	827	17560
Elev1	Mean basin elevation	m	50	1226	2810
Pminsum	10 th percentile of summer monthly precipitation	mm/month	55	69	83
Pavgapr	Average April precipitation	mm/month	68	92	116
Tmaxfal	90 th percentile of fall monthly temperature	K	287.4	291.7	296.3
OMH	Soil organic matter content	% by weight	1.49	5.40	19.55

Sample Characteristics

The 160 gauged watersheds comprising the sample represent a population of natural, unimpaired streams in the Mid-Atlantic US. Locations of each gauge are depicted in Figure 1. The gauges are scattered among 78 USGS Hydrologic Unit Codes (HUCs). 45% of the HUCs have only one gauge and 73% have two or fewer. Figure 1 shows a concentration of 18 gauges on the border of New Jersey and New York. These gauges are located in the linked watersheds: the East Branch Delaware, Upper Delaware, and Middle Delaware-Monquap-Broadhead watersheds. With the occurrence of multiple

gauges within the same HUC or in a series of linked HUCs, spatial correlation may exist; therefore, there is potential for correlated streamflows in the sample.

Low-Flow Regression

To predict the $Q_{7,10}$ of gauged sites, a regression equation can be used that represents the relationships between the $Q_{7,10}$ and a watershed's physiographic and climate characteristics. The typical form of this relationship is

$$Q_{7,10} = \alpha \prod_{i=1}^n \chi_i^{\beta_i} \quad (1)$$

where the $Q_{7,10}$ is the low-flow statistic, χ_i is the i th of n drainage basin characteristics, and α and β_i are model parameters. Taking the log of both sides produces a linear equation whose parameters can be fit using stepwise linear regression. Akaike's Information Criterion (AIC) (Burnham and Anderson, 2002) was then used to compare alternative models with different numbers of explanatory variables. In addition, cross-validation studies were conducted to assess the sensitivity of the final explanatory variables to variations in the gauge site sample.

Stepwise Regression

The forward stepwise regression procedure, with a 5% significance level for entering variables, was used to model the $Q_{7,10}$ from the entire sample. This procedure can result in multi-collinearity problems. To address this, the variance inflation factor (VIF) was used to identify individual explanatory variables with multi-collinearity problems, as indicated by a VIF greater than ten (Rawlings *et al.*, 1998). Explanatory variables with high VIFs and physical explanations for possible collinearity problems were grouped as pairs. Two pairs of climate variables displayed possible multi-collinearity problems: the 90th percentile for fall maximum temperature (Tmaxfal) with the 90th percentile for spring minimum temperature and the average July precipitation with the 10th percentile for average monthly summer precipitation (Pminsum). Finally, to achieve smaller VIF values, one pair was removed from the regression, and the explanatory variables from that pair were added individually. The variable contributing to the highest coefficient of determination from each pair was selected; Tmaxfal and Pminsum contributed to the highest coefficients of determination and were included in the fitted model.

The resulting fitted model is given by:

$$Q_{7,10} = 3.73 * 10^{71} DA^{0.87} Kb2^{49.25} Pminsum^{1.74} Pavgapr^{2.30} Tmaxfal^{-34.86} OMH^{0.29} Elev2^{0.21} \quad (2)$$

The log-linear form of Equation 2 has an adjusted coefficient of determination of 0.936 and a mean square error of 0.175, with all parameters significant at $p < 0.001$. Drainage area (DA) and Kb2 account for the majority of the incremental explained variation, 65% and 21%. The climatic variables Pavgapr and Tmaxfal account for 5% and 2%, whereas the remaining variables account for less than 1%. Although Equation 2 has a relatively

high adjusted coefficient of determination, a model with fewer explanatory variables and high explanatory power is preferred. To select the smallest number of explanatory variables necessary to represent the data, additional models with fewer variables were created and tested using the AIC. The AIC quantifies the extra explanatory power of a model gained by an extra variable (Burnham and Anderson, 2002) and is equal to

$$AIC = n \ln(\sigma^2) + 2k \quad (3)$$

where n is the number of observations, σ^2 is the mean square error, and k is the number of parameters including the intercept. The best three candidate models are described in Table 4, which lists the explanatory variable parameter estimates, standard errors, adjusted coefficients of variation, mean square errors, and the associated AICs. Set I are the variables in Equation 2 with subsequent sets consisting of subsets of I. Variables were removed in reverse order of F statistic value from the stepwise procedure. Models with low AICs are preferred, and those with an AIC within 2 units of the full model given by Equation 2 (as indicated in Table 4 by ΔAIC) are candidate models (Burnham and Anderson, 2002).

Table.4. Comparison of Variable Set Coefficients and Characteristics

Parameter Estimates of Explanatory Variables			
Explanatory Variables	Variable Set		
	I	II	III
DA	0.87	0.98	0.98
Kb2	49.25	49.95	50.42
Pavgapr	1.74	2.24	2.55
Tmaxfal	-34.86	-35.71	-29.65
Pminsum	1.74	1.57	1.65
OMH	0.29	0.27	X
Elev2	0.21	X	X
Standard Errors of Parameter Estimates			
Explanatory Variables	Variable Set		
	I	II	III
DA	0.06	0.03	0.03
Kb2	2.22	2.22	2.35
Pavgapr	0.31	0.31	0.32
Tmaxfal	5.87	5.93	6.1
Pminsum	0.45	0.44	0.47
OMH	0.06	0.06	X
Elev2	0.09	X	X
Model Characteristics			
	Variable Set		
	I	II	III
Adj R2	0.936	0.935	0.927
MSE	0.175	0.18	0.202
AIC	-260.4	-258.5	-242.2
ΔAIC	0	1.9	18.2

Variable set II was selected as the final model and takes the form

$$Q_{7,10} = 1.80 * 10^{74} DA^{0.98} Kb2^{49.95} Pminsum^{1.57} Pavgapr^{2.24} Tmaxfal^{-35.71} OMH^{0.27} \quad (4)$$

The log linear form of the model in Equation 4 has a high adjusted coefficient of determination of 0.935, a mean square error of 0.18, an AIC within 2 units of Equation 2, with all parameters significant at $p < 0.001$.

The explanatory variables in Equation 4 represent relationships with physical interpretations. For example, the $Q_{7,10}$ increases with increasing drainage area due to the larger area for precipitation recharge. The $Q_{7,10}$ also increases as summer and April precipitation increases, as the recession coefficient increases due to steadier baseflow, and as % organic matter increases due to increased holding capacity and conductivity. The $Q_{7,10}$ decreases as fall temperature increases due to evapotranspiration.

To confirm the selection of variables, separate stepwise regressions on eight randomly generated half samples were compared to the whole sample results. The explanatory variables from the whole-sample regression model appeared most frequently of all half-sample variables. Variables DA and KB2 were statistically significant explanatory variables in all eight half samples, OMH in seven, and variables of summer precipitation, spring precipitation, and fall temperature in more than half. In addition, the final model in Equation 4 was used to model each half sample; all samples displaying adjusted coefficients of determination greater than 0.92.

Future Low-Flow Predictions

The model in Equation 4 is used in two forms to predict possible future changes in the $Q_{7,10}$. First, individual $Q_{7,10}$ predictions and prediction intervals were estimated for each gauge using watershed specific values except for the three climate variables: Tmaxfal, Pavgapr, and Pminsum. Inputs for these climate variables were estimated from the changes predicted by the GCMs from the IPCC Regional Scatter Diagrams (2004). Although topographical characteristics of individual watersheds modify the regional predictions (Giorgi *et al.*, 2003), uniform, regional climatic changes were applied to all gauges without downscaling in this study.

The three climatic variables in Equation 4 don't match exactly the available IPCC data. Therefore, the changes in the average April precipitation (Pavgapr), 10th percentile for precipitation for period June-August (Pminsum), and 90th percentile maximum temperature for September-November (Tmaxfal) are assumed to be the same as the IPCC changes in average seasonal precipitation and temperature in Tables 1 and 2. This is equivalent to assuming that the monthly and seasonal precipitation variables are multiplied by a constant factor, e.g., 1.1 for a 10 percent increase, while the entire distribution of monthly and seasonal temperatures is shifted (generally upward) by a fixed amount.

Equation 4 is used to predict both current and future values of the $Q_{7,10}$, and can be used to predict the ratio of the $Q_{7,10}$ at some future time $Q_{7,10}^2$ and the current $Q_{7,10}^1$ (assuming the watershed physiographic variables and the baseflow recession constant remain the same):

$$\frac{Q_{7,10}^2}{Q_{7,10}^1} = \left(\frac{P_{minsum}^2}{P_{minsum}^1}\right)^{1.57} \left(\frac{P_{avgapr}^2}{P_{avgapr}^1}\right)^{2.24} \left(\frac{T_{maxfal}^2}{T_{maxfal}^1}\right)^{-35.71} \quad (5)$$

Equation 5 translates relative changes in climate variables to relative changes in the $Q_{7,10}$.

Low-Flow Prediction Results

Using Equation 4, future $Q_{7,10}$ predictions were estimated for each gauge based on the climate predictions described in Tables 1 and 2. A summary of the average percentage change in the $Q_{7,10}$ from baseline for each model is presented in Table 5 for Scenario A2 and Table 6 for Scenario B2. For all scenarios, GCMs, and time periods, except CSIRO in time period 2010-2039 for Scenario A2, the $Q_{7,10}$ is estimated to decrease, even with increasing precipitation. The GFDL model generally predicts the most severe change due to large decreases in precipitation; conversely, CSIRO anticipates less change in the $Q_{7,10}$ in A2, due to the model's large increases in precipitation.

Table.5. Average Predicted % Change in Q_{710} for Each Climate Model (Scenario A2)

Model	Time Period		
	2010-2039	2040-2069	2070-2099
CSIRO	5.40%	-7.20%	-14.60%
HADC	-7.80%	-18.40%	-16.50%
CGCM	-12.70%	-25.80%	-34.00%
GFDL	-20.00%	-35.90%	-45.20%

Table.6. Average Predicted % Change in Q_{710} for Each Climate Model (Scenario B2)

Model	Scenario B2		
	Time Period		
	2010-2039	2040-2069	2070-2099
CSIRO	-2.30%	-7.90%	-10.60%
HADC	-7.00%	-3.70%	-6.60%
CGCM	-18.00%	-14.00%	-21.90%
GFDL	-10.10%	-33.20%	-47.90%

To see if future climate predictions are extrapolative, Figure 2 compares the range within the sample of climatic variables used for future prediction with the baseline climate conditions. As shown, there is still a significant degree of overlap for these variable ranges, even for the cases where the variables are shifted maximally among the models

considered. For this reason, the streamflow predictions generated by this model are (at least considering each variable individually) for the most part interpolative, and the climate predictions do not represent radically different or new climatic regimes.

There is considerable uncertainty associated with the GCMs' predictions. Equation 5 was used to perform a parametric sensitivity analysis of the $\% \Delta Q_{7,10}$ to changes in the climate variables. In Figure 3, contour lines represent estimates of the $\% \Delta Q_{7,10}$ over a range of $\% \Delta P_{minsum}$ and $\% \Delta P_{avgapr}$ changes, as indicated by the x and y axis in each panel. The extremes on the x and y axes are the largest changes predicted for any single weather station in the region using statistical downscaling of the GCM predictions (Graham, 2004). The six panels represent different increases in Tmaxfal from baseline.

As Equation 5 indicates, the $\% \Delta Q_{7,10}$ becomes increasingly negative as temperature increases. The shift of the 0 contour line for $\% \Delta Q_{7,10}$ up and to the right as temperature increases exemplifies this relationship. With the largest temperature change, indicated by the 5 K temperature panel, the 0 contour line for $\% \Delta Q_{7,10}$ is shifted the farthest to the right, where almost all possible future precipitation changes result in a decrease in the $Q_{7,10}$. Without considering individual GCM climate predictions, the model predicts future decreases in the $Q_{7,10}$ for both increases and decreases in future precipitation when future fall temperature increases.

The GCM Scenario A2 prediction results also support the finding that the $\% \Delta Q_{7,10}$ becomes increasingly negative as temperature increases. For example, the CSIRO model in time period 2010-2039, as indicated by a white star in Figure 3, predicts approximately a 1 K change in summer temperature; therefore, the symbol for this model and time combination lies in the 1 K temperature panel. For this nearest time period, the symbol falls near the 0 contour line for the $\% \Delta Q_{7,10}$. CSIRO's prediction in the 2040-2069 time period, as indicated by the gray star, lies in the 3 K temperature panel. With this increase in temperature, the star now falls below the 0 contour line for the $\% \Delta Q_{7,10}$, indicating a decrease in the $Q_{7,10}$. Similarly, in time period 2070-2099, the CSIRO prediction for temperature increases and the model lies in the 5 K temperature panel with the star falling near the -25% contour line for the $\% \Delta Q_{7,10}$. For models with temperature change predictions falling between the temperature panel changes, such as HADCM3 in period 2010-2039 with a 1.5 K change, the symbol is depicted on the two panels that bound the predicted temperature change. The remaining three models show trends similar to CSIRO's of decreased $Q_{7,10}$ as time period and temperature increase.

Low-Flow Water Quality Ratios

A mass-balance model allows evaluation of the impact of multiple climate change scenarios on the TMDL allocation of a primary constituent through changes in the $Q_{7,10}$.

Based on this mass balance model, the ratio of future TMDL to current TMDL to meet a specified in-stream waste concentration is given by the ratio of future to baseline $Q_{7,10}$:

$$\frac{TMDL_{future}}{TMDL_{current}} = \frac{Q_{7,10}^{future}}{Q_{7,10}^{baseline}} = \frac{\% \Delta Q_{7,10}}{100} + 1 \quad (6)$$

where the $Q_{7,10}$ is predicted by the statistical model. For cases where the $Q_{7,10}^{future}$ is less than $Q_{7,10}^{baseline}$ (as in most predictions from our model), TMDL's designed to meet current water quality standards may fail to do so in the future.

Low-Flow Water Quality Prediction Results

Low-flow percent change predictions for climate change Scenario A2 were calculated using Equation 5 and applied to Equation 6 to determine the fraction of current TMDL allowed in the future to meet water quality criteria when considering the influence of climate change on low flow. Figure 4 shows the ratio of future TMDL to current TMDL, which can also be interpreted as the ratio of the future to baseline $Q_{7,10}$. Figure 4 also shows the 5th and 95th percentile estimates for each climate model and time period.

The 5th and 95th percentile values were estimated using a Latin hypercube simulation (Neter *et al.*, 1996) of the three climate parameter estimates β_i in Equation 4 using the standard errors from Variable Set II in Table 4 as well as accounting for the covariance of the estimated β_i . A comparison of the estimated (calculated when fitting the model in Equation 4) and simulated correlation coefficients of the β_i pairs is presented in Table 7.

Table.7. Estimated Correlation Matrix for Coefficients of Model Explanatory Variables with Original Sample Correlations in Parenthesis

Correlation Matrix			
	Pavgapr	Pminsum	Tmaxfal
Pavgapr	1.000		
Pminsum	-0.114 (-0.103)	1.000	
Tmaxfal	0.248 (0.249)	0.240 (0.234)	1.000

In Figure 4, a value of 1.0 represents a future TMDL equivalent to the current allocation, where values less than one indicate a required decrease in future TMDL. All predicted ratios are smaller than 1.0 in the figure, except for model CSIRO in 2010-2039. Only CSIRO and HADC results have 95th percentile values greater than 1.0. In the earliest future time period, the predictions of the four models indicate that the ratio of future to current TMDL could range from 0.8 to above 1.0.

Discussion

This study presents a first estimate of future changes in low flows and the resulting effect on water quality for a range of possible climatic changes. Under Scenarios A2 and B2, the regression model predicts a decrease in the future $Q_{7,10}$ for the Mid-Atlantic region; still, despite improvements in spatial datasets as emphasized by Kroll et al. (2004) and Smahtkin (2001), future $Q_{7,10}$ predictions from the regression model are highly uncertain. Future predictions are additionally complicated by uncertainty in climate predictions.

The GCM predictions differ in the direction and severity of predicted climate change for this region. The IPCC (2004) advises that no single model is preferable for a particular region, leaving a wide range of possible future climate predictions. To further complicate GCM applications, the predictions are not probabilistic, but based on possible storylines or scenarios. In this study, Scenarios A2 and B2 are presented; other scenarios could result in smaller $Q_{7,10}$ changes. Without probabilistic scenarios, future climate predictions are difficult to incorporate into quantitative water quality planning analysis.

Despite uncertainty in predictions of low flow, the potential decrease in low flow has implications for the TMDL allocation process. Change in low flow could affect both the identification of impaired waterbodies as well as the TMDL allocation.

Identifying Impaired Waterbodies

Future decrease in low flow could increase the number of waterbodies that fail to meet ambient water quality criteria. In particular, decreases in low flow, in combination with the increases in temperature as evaluated by Morrill *et al.* (2005), could increase the number of violations for no-exceedance criteria, criteria that must be met at all times (NRC, 2001). This would result in additional streams requiring TMDL assessment. In states with standards that specify that criteria do not apply during low streamflows, the acute effects of pollution could become more severe.

TMDL Planning

Future changes in low flow also have implications for TMDL planning. Once a waterbody is categorized as impaired, TMDLs are set based on empirical or mechanistic modeling. Federal regulation requires each state to determine a schedule for TMDL development; these schedules should plan for all TMDLs to be established in no more than 8 to 13 years (40 CFR 130.7(d)(1)). This TMDL development time is comparable to the near-future climate change time period. Therefore, in the time between identifying a water as impaired and TMDL development, climate change could invalidate the meteorological assumptions in the TMDL model and require a reassessment. However, water quality modeling is costly and time-consuming, and the cost of adding climate scenarios may outweigh the benefit of preventing reassessment, especially given the uncertainty in the GCM predictions. When GCM climate predictions improve, climate scenarios may be most effective at locations where severe climate change is anticipated.

Overall, GCMs predict the least change in climate for the US in the Mid-Atlantic region (NAST, 2001). In addition, this region experiences the least streamflow variability of all

the U.S. regions (Hurd *et al.*, 1999). Climate scenarios are most important for watersheds in regions such as the Great Plains, where the most severe climate change is anticipated and baseflow is relatively low (Hurd, 1999; NAST, 2001). Considering future climate scenarios in the Great Plains region –through a dynamic, site-specific model that combines dilution effects with possible changes in temperature, kinetic reaction rates, and nonpoint-source loading - may prevent TMDL reassessments.

Conclusions

The principal conclusions from this study include:

- Model predictions indicate decreases in low flow as a result of climate change for the Mid-Atlantic region, even with predicted increases in precipitation,.
- A simple low-flow water quality model for a primary pollutant predicts required decreases for future point-source TMDLs under most future climate scenarios.
- Future improvements in both climate and streamflow models could allow consideration of future climate change scenarios in the TMDL development process.

Acknowledgements

Support for this project is provided by the Global Change Research Program, Office of Research and Development, U.S. Environmental Protection Agency (Cooperative Agreement R-83053301). We would like to thank our partners from The Consortium for Atlantic Regional Assessment (CARA), especially Steve Graham. We would also like to thank Mike Haire at the EPA Office of Wetlands, Oceans, and Watersheds.

References

- Arnell N.W. (2003). Relative Effects of multi-decadal climatic variability and changes in the mean and variability of climate due to global warming: future streamflows in Britain. *Journal of Hydrology*, 270, 195-213.
- Burnham, K.R. and D.R. Anderson. (2002). *Model selection and multimodel inference*. New York: Springer.
- Clean Water Act of 1987. (1987). Alexandria, VA: W.P.C.F.
- Dingman, S.L., and Lawlor, S.C., (1995). Estimating low-flow quantiles from drainage-basin characteristics in New Hampshire and Vermont. *Water Resources Bulletin*, 31(2), 243-256.
- Eheart, W.J., Wildermuth, A.J, and Herricks, E.E. (1999). The Effects of Climate Change and Irrigation on Criterion Low Streamflows used for determining total maximum daily loads. *Journal of the American Water Resources Association*, 35, 1365-1372.
- Giorgi, F., Mearns, L.O., and Whetton, D. (2003). Guidelines for Use of Climate Scenarios Developed from Regional Climate Model Experiments. http://ipcc-ddc.cru.ueq.ac.uk/guidelines/dgm_no1_v1_10-2003.pdf.
- Graham, S. (2004) Consortium for Atlantic Regional Assessment: NCDC best climate estimates. Personal email.
- Hurd, B., Leary, N., Jones, R., and Smith, J. (1999). Relative Regional Vulnerability of Water Resources to Climate Change. *Journal of the American Water resources Association*, 35, 1399-1409.

- IPCC. (2000). *Special Report of the Intergovernmental Panel on Climate Change: Emission Scenarios*. Cambridge, UK: Cambridge University Press.
- IPCC data distribution centre (ddc). (2004). Future climate in world regions: an intercomparison of model-based projections for the new IPCC Emissions Scenarios (Regional Scatter Diagrams). http://ipcc-ddc.cru.uea.ac.uk/sres/scatter_plots/scatterplots_region.html
- Kroll, C.N., Luz, J.G., Allen, T.B., and Vogel, R.M. (2004). Developing a watershed characteristics database to improve low streamflow prediction. *Journal of Hydrologic Engineering*, 9(2), 116-125.
- Lettenmaier, D.P., Wood, A.W., and Palmer R.N. (1999). Water resources implications of global warming: A US regional perspective. *Climate Change*, 43(3), 537-579.
- Morrill, J., Bales, R.C., and Conklin, M.H. (2005). Estimating stream temperature from air temperature: implications for future water quality. *Journal of Environmental Engineering*, 131(1), 139-146.
- National Assessment Synthesis Team. (2001). *Climate change impacts on the United States: the potential consequences of climate variability and change* (Report for the US Global Change Research Program). Cambridge, UK: Cambridge University Press.
- National Research Council. (2001). *Assessing the TMDL approach to water quality management*. Washington, D.C.: National Academy Press.
- Neter, J., Kutner, M.H., Nachtsheim, C., and Wasserman, W. (1996). *Applied Linear Statistical Models* (4th Ed.). Chicago: Irwin.
- Nijssen, B., O'Donnell, G.M., and Hamlet, A.F. (2001). Hydrologic sensitivity of global rivers to climate change. *Climate Change*, 50(1-2), 143-175.
- Rawlings, J. O., Pantula, S. G., and Dickey, D. A. (1998). *Applied regression analysis: A research tool* (2nd Ed.). New York: Springer.
- Rifai, H.S., Brock, S.M., and Ensor K.B. (2000). Determination of low-flow characteristics for Texas streams. *Journal of Water Resources Planning and Management-ASCE*, 126(5), 310-319.
- Slack, J.R., Lumb, A.M., and Landwehr, J.M. (1993). *Hydro-climatic data network (HCDN): A U.S. Geological Survey streamflow data set for the United States for the study of climate variations, 1874-1988*. (U.S. Geological Survey Water Resources Investigation Rep. 92-129). Reston, VA: U.S. Geological Survey.
- Smakhtin, V.U. (2001). Low flow hydrology: a review. *Journal of Hydrology*, 240(3-4), 147-186.
- Tallaksen, L.M. (1995). A review of baseflow recession analysis. *Journal of Hydrology*, 165(1), 349-370.
- Vogel, R.M., and Kroll, C.N. (1996). Estimation of baseflow recession constants, *Water Resources Management*, 10(2), 303-320.
- Wiley, J. and Curran, J. (2003) *Monthly and seasonal low-flow statistics for ungauged sites on streams in Alaska and Conterminous basins in Canada* (Water Resources Investigations Report 03-4114). Anchorage, AL: U.S. Geological Survey.
- Zecharias, Y.B., and Brutseart, W. (1988). Recession characteristics of groundwater outflow and base flow from mountainous watersheds. *Water Resources Research*, 24(10), 1651-1658.

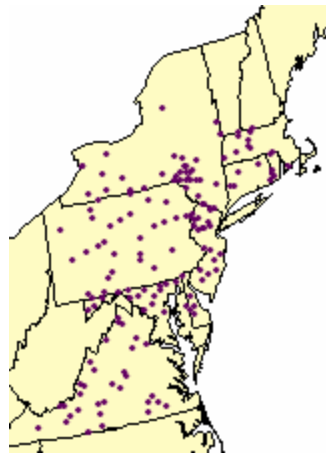


Figure 1. Location of USGS Stream Gauges Used in Study

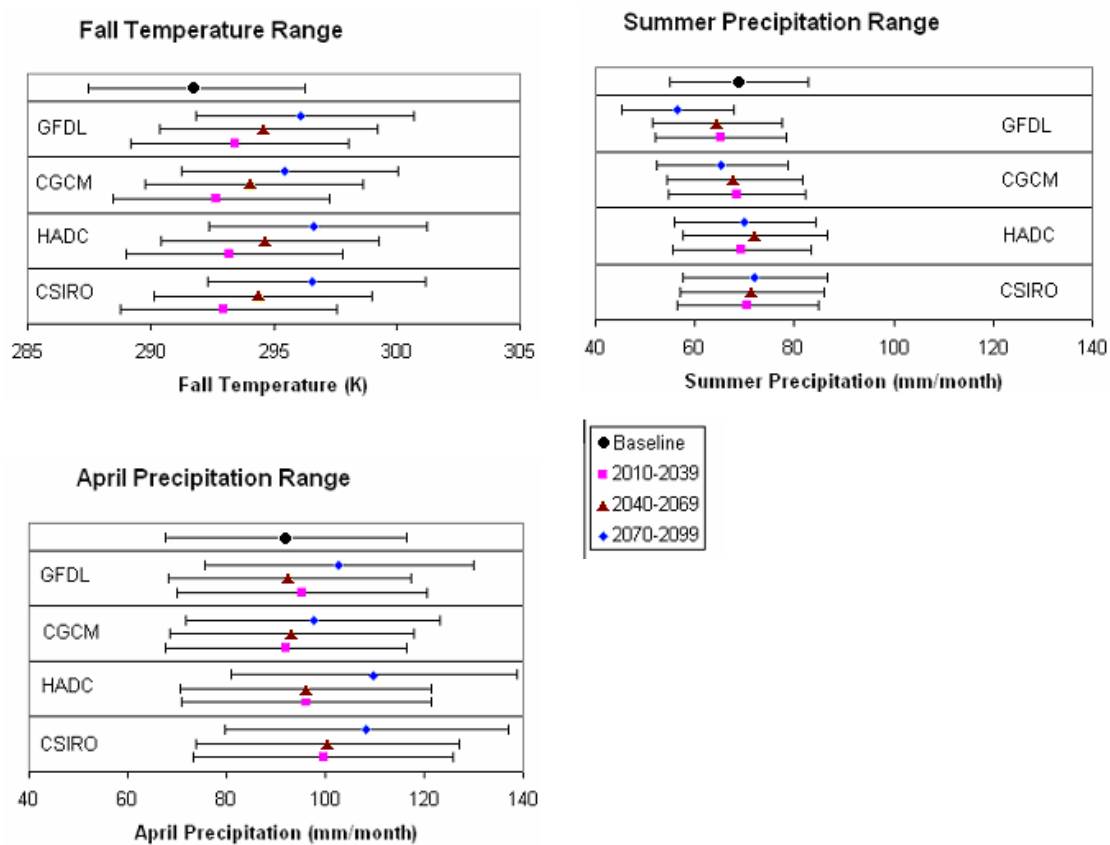


Figure 2. Comparison of Baseline Climate to Future Predicted Climate

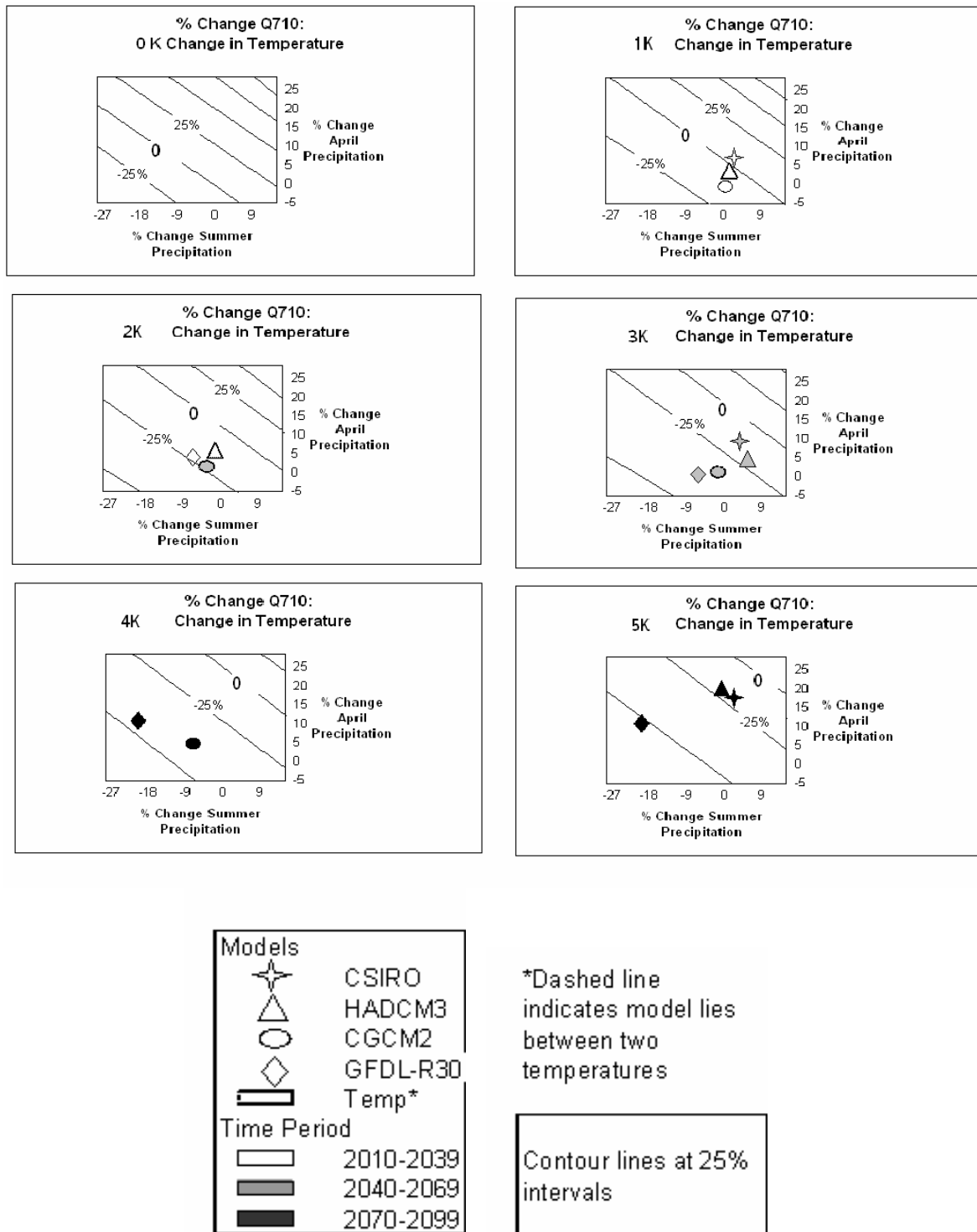


Figure 3. Percentage Change in Predicted Low Flow for Different Combinations of Changes in Future Temperatures and Precipitation with Associated GCM Prediction

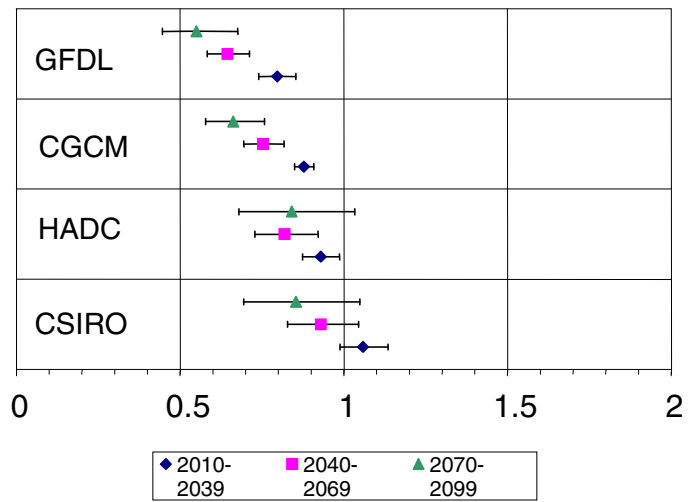


Figure 4. Predicted Average, 5th, and 95th Percentiles of Ratio of Future TMDL to Current TMDL or Future 7Q10 to Baseline 7Q10 Ratio